Conformation Analysis of Carotenoids in the Purple Bacterium *Rhodobium marinum* Based on NMR Spectroscopy and AM1 Calculation†

Pu Qian,*,‡,§ Tadashi Mizoguchi,‡ Ritsuko Fujii,‡ and Kazukimi Hara‡

Faculty of Science, Kwansei Gakuin University, Uegahara, Nishinomiya 662-8501, Japan, and Krebs Institute for Biomolecular Research, Department of Molecular Biology and Biotechnology, The University of Sheffield, Firth Court, Western Bank, Sheffield S10 2TN, U.K.

Received March 29, 2002

Five carotenoids existing in the purple bacterium of *Rhodobium marinum*, lycopene, anhydrorhodovibrin, spirilloxanthin, rhodopin, and rhodovibrin, were isolated and purified. Their configurations in the chromophore region and conformations of the terminal part were determined by 1D, 2D ^{1}H and ^{13}C NMR spectroscopy. The semiempirical quantum chemical calculation AM1 was subsequently performed using the rough 3-D structures established by NOE correlations as an initial input. The final optimized structures are coincident with ^{1}H-^{1}H NOE correlations and match with the X-ray crystallographic data of carotenoids. The calculation results show that chemically symmetrical carotenoids have a C_i point group. The C_i point group of molecules was destroyed by asymmetrical terminal part although the polyene chain still keeps it roughly. The polyene region of investigated carotenoids are in all-*trans* with slightly twisted in-plane and slight out-plane forming s-shape carbon backbone due to the spatial interaction of the methyl groups. Terminal parts, on the other hand, have several stable conformers due to the freely rotatable single bonds, but they prefer to take extended conformations.

1. INTRODUCTION

Carotenoids in the photosynthetic bacteria play at least three major functions.[1] The first one is light-harvesting function. These molecules can collect light energy, mostly in the blue-green region, in which the light absorption efficiency of bacteriochlorophyll is very low. The absorbed energy is then transferred to reaction center (RC), at which the charge separation takes place and light energy is transferred into chemical energy. The second function is so-called light-protection. Carotenoids protect the photosynthetic organism from damage by quenching excited state molecules of bacteriochlorophyll and singlet state of oxygen molecules. Also, the carotenoids are considered as a structural component that stabilizes the light-harvesting complexes. It is obvious that the detailed structural information on carotenoids is absolutely necessary for understanding their functional mechanisms in the photosynthetic procedures.

The purple photosynthetic bacterium *Rhodobium (Rh.) marinum* was first reported by J. F. Imhoff.[2] It only contains RC/LH1 as a sole light-harvesting complex. This ring-like protein complex[3,4] as well as its individual components, RC and LH1, can be purified respectively.[5] Pigment analysis results show that five different C_{40} carotenoids are present, which belong to a so-called "normal spirilloxanthin" biosynthetic pathway,[6,7] bound to protein complexes. They are lycopene, anhydrorhodovibrin, spirilloxanthin, rhodopin and rhodovibrin. The relative percentage of each carotenoid is time dependent during the growth of cell.[8] To investigate the functions of carotenoid in the photosynthetic processes, we need to know the detailed structural information of carotenoids involved in process both free in solvent and bound in protein complexes.

Several methods can be used to obtain 3-D structural information of carotenoids. One of the most reliable methods is X-ray crystallography. Unfortunately, getting well-formed carotenoid crystals is always a difficult task because most carotenoids are very sensitive to light, heat, air, acid and so on. They are easy to degrade before forming good enough crystals. Furthermore, with the increase in the number of conjugated C═C bonds n (e.g. n = 12 or 13), (e.g. refs 12 and 13), carotenoid molecules becomes easier to be isomerized and decomposed, and their solubility in organic solvent decreases. These also increase the difficulty for sample preparation and crystallization. That is why few X-ray crystallographic data of carotenoids are available so far.

With the development of nuclear magnetic resonance (NMR) spectroscopy, it has been become one of the most powerful tools for the identification and structure elucidation of carotenoids in the past decades.[9] The increase of measuring frequency greatly simplifies the interpretation of NMR spectrum since the chemical shift difference, measured in Hz, among different signals having different shielding constants, increases proportionally to the measuring frequency. Combined with one-dimensional and two-dimen-

* Corresponding author phone: 44-114-2222739; fax: 44-114-2728697; e-mail: p.qian@sheffield.ac.uk. Present address: Department of Molecular Biology and Biotechnology, University of Sheffield, Firth Court, Western Bank, Sheffield S10 2TN, U.K.

† Abbreviation**:** 3-D, three dimension; $1^1B_u^+$, group theory symbol of carotenoid first excited state; $1^1A_g^-$, group theory symbol of carotenoid ground state; AM1, Austin model 1, C_i, a symbol of central symmetry; *Rh, rhodobacter*; COSY, correlation spectroscopy; DEPT, distortionless enhancement by polarization transfer; HSQC, heteronuclear single quantum coherence; HMBC, heteronuclear multi quantum coherence; LH1, light harvesting complex 1; LPLC, low-pressure liquid chromatography; MM, molecular mechanics; NOE, nuclear Overhauser effect; RC, reaction center; RMS, root-mean-square; ROESY, rotating-frame Overhauser enhancement spectroscopy; S/N, ratio of signal/noise.

‡ Kwansei Gakuin University.

§ University of Sheffield.

10.1021/ci0255230 CCC: $22.00 © 2002 American Chemical Society
Published on Web 10/05/2002

sional (1D and 2D) techniques, many complicated NMR spectra of carotenoid both for proton and ^{13}C can be assigned ambiguously.[10] It is indubitable that NMR is one of the most powerful structure research tools for carotenoids because NMR techniques not only provide information on the connectivity of atoms but also their spatial correlation in a molecule. By the use of ^1H COSY and (^1H,^{13}C) heteronuclear COSY NMR spectra, connectivity of carbon atoms can be established, while the NOE relationship provides spatial structure information, with which a rough 3-D molecular structure of carotenoid in solution can be constructed although it cannot provide structure parameters such as bond length, bond angle and dihedral angle accurately.

Another useful method is quantum chemical calculation. Several successful calculations on carotenoids have been published during the past decade.[11−13] The calculation results of β-carotene and canthaxanthin[13] based on the AM1 method correspond well with their X-ray crystallographic data indicating that semiempirical quantum chemical calculation on carotenoid is feasible. It is worth noting that a reasonable initial input structure, which can avoid local minima, is one of the key points to get reliable results of the calculation. Combination of NMR and quantum chemical calculation might be an ideal way to get reliable structural information of carotenoid in the solution, because the former can provide rough 3-D structure information, which reflects the actual states of molecule in solution, while the later can provides accurate structural parameters.

In the present work, we isolated the main carotenoids from the whole cell of *Rh. marinum*. Each carotenoid was purified by chromatography and recrystallization. Based on the ^1H and ^{13}C NMR experimental results, their initial input structures for semiempirical quantum chemical calculations of AM1 were constructed. The corresponding 3-D geometry of carotenoid was then calculated using the AM1 method. Based on the optimized geometry, other possible stable conformers were obtained by rotating terminal-parts of carotenoid molecule.

2. MATERIALS AND METHODS

2.1. Cell Growth Conditions. Cells of *Rh. marinum* were cultured at 30 °C anaerobically in the modified DSM-27 Rhodospirillaceae medium.[14] Cells were harvested by centrifugation after 4-day culture and stored at −20 °C under nitrogen atmosphere before use.

2.2. Extraction and Purification of Carotenoids. Carotenoids in the *Rh. marinum* were extracted from whole cells. Initially, 100 g wet cells were suspended in 200 mL of 20 mM pH 8.0 Tris-HCl buffer for homogenization. Buffer solution in it was removed by centrifugation. The hydrated cells were extracted with 200 mL of mixed organic solvent of acetone and methanol (7:3 v/v). The mixture was stirred for 30 min under constant bubbling of nitrogen in dark. After centrifugation separation (3000g, 4 °C, 30 min), the supernatant was pooled, and the debris was extracted again until colorless. Combined supernatant that contains mixed pigments was evaporated in a vacuum to dryness and dissolved in a minimum volume of benzene. The mixed pigments were separated by the use of a silica gel open column (d = 30 mm, h = 100 mm) Wakogel C-300, Japan with eluent of 2.5% acetone in benzene (v/v). Bacteriochlorophyll *a* and its derivatives were trapped in the column, and the five colored bands, corresponding to five different carotenoids, were collected. They were passed through the second silica gel open column (d = 30 mm, h = 20 mm) Wakogel C-300, Japan, which was developed with 100% benzene individually. All-trans lycopene, rhodopin and rhodovibrin were further purified by crystallization in *n*-hexane. The all-*trans* spirilloxanthin and anhydrorhodovibrin were purified by low-pressure liquid chromatography (LPLC) as follows. The coarse spirilloxanthin was loaded on the LPLC column (d = 40 mm, h = 300 mm) packed with $Ca(OH)_2$ (Junsei chemical Co., Ltd., Japan), which was developed with benzene containing 40% acetone under 2 kg/cm^2 constant pressure. Well-separated all-*trans* spirilloxanthin was recrystallized in the mixed solvent of acetone and benzene (1:5 in v/v). A similar method was applied for obtaining all-*trans* anhydrorhodovibrin with the modification of LPLC conditions: benzene with 20% acetone as eluent; recrystallization in the mixed solvent of THF and *n*-hexane (1:5 in v/v). Above procedures were repeated several times to accumulate enough samples for good S/N NMR spectra. Due to the low percentage of rhodovibrin in the cell and its strong polarity, we have not obtained a large enough amount of pure rhodovibrin sample for its ^{13}C NMR measurements.

2.3. ^1H and ^{13}C Nuclear Magnetic Resonance Spectroscopy. The 400 MHz ^1H NMR and ^{13}C spectra of each carotenoid were recorded in chloroform-d_1 (ISOTEC Inc., 99.8% D) by the use of a JEOL JNM-A400 FT NMR spectrometer; tetramethylsilane was used as an internal standard. A set of one-dimensional spectrum (digital resolution 0.24 Hz, obfrq = 399.65 MHz, pules angle = 90° with pw = 10.60 ms) and two-dimensional ^1H-^1H COSY (correlation spectroscopy) and ^1H-^1H ROESY (rotating-frame Overhauser enhancement spectroscopy) spectra (digital resolution, 6.64 Hz) were recorded for each sample in $CDCl_3$ solution. The pulse sequence was as follows: ^1H-^1H COSY, 90-t_1-90-t_2, and ^1H-^1H ROESY, 90-t_1-t_m (spin-lock)-t_2 with t_m = 250 ms. In the case of ^{13}C NMR measurement, more than 5 mg of sample of each carotenoid was used to get a good enough S/N spectrum except for rhodovibrin. 1-D ^{13}C spectrum with ^1H BB (broad-band) decoupling as well as a set of DEPT (distortionless enhancement by polarization transfer) spectra (digital resolution, 0.83 Hz; obfrq, 100.40 MHz, scan time, 2000) with the variable pules angle ($\Theta_{y'}$) of 45°, 90°, and 135° were recorded according to the following pules sequences: ^1H channel: $90^\circ_{x'} - \tau - 180^\circ_{x'} - \tau - \Theta_{y'} - BB$; ^{13}C channel: $90^\circ_{Y'} - \tau - 180° - \tau - FID(t_2)$. A set of 2-D hetronuclear correlated NMR spectra including C,H−COSY, HSQC (heteronuclear single quantum coherence) and HMBC (heteronuclear multi quantum coherence) were also recorded for the same samples.

2.4. Calculation Methods. The initial configurations of the conjugated region and conformations of the terminal part (the part out of the conjugated region) were built based on the ^1H-^1H NOE correlation signals and standard geometrical parameters. The established structure was subsequently optimized with molecular mechanics force field program MM+, which has extensions of molecular mechanics method initially described by Kao et al.[15] The optimized structure was then fed to a semiempirical quantum chemical calculation program AM1. The final minimum heat of formation was obtained by simultaneous relaxation of all geometrical

parameters until the minimum RMS gradient was less than 0.005.

To search stable conformations of carotenoid, a specified dihedral angle in terminal-parts was rotated between 0° and 360° with a 5° interval. The geometry optimization of each step was performed with a rotated dihedral angle fixed as a parameter and freedom of all other degrees. To shorten computational time, gradient norm equaling to 0.1 was set as a convergence condition.

3. RESULTS AND DISCUSSIONS

3.1. Purity of Carotenoids. As stated above, the initial structure of carotenoid molecule for calculation was established mainly by the ^{1}H-^{1}H NOE signals. It is obvious that having a pure enough carotenoid sample that is both free from the contamination of other carotenoids and its isomers is one of the key steps of this work. The purity of involved carotenoids was double checked by HPLC and UV−vis spectra. The HPLC conditions used for anhydrorhodovibrin and spirilloxanthin are as follows: column (4.6 × 300 mm) packed with calcium hydroxide; 1.6% acetone in benzene at 0.6 mL/min flow rate as eluent; 480 nm detection. For other carotenoids, another HPLC analytical system was employed: Column, Lichrosorb Si-60 (d = 4.6 mm, h = 300 mm); eluent, acetone containing 0.05% *N*-ethyldiisopropylamine, detection wavelength was set at 480 nm. The relative purity of spirilloxanthin, anhydrorhodovibrin, lycopene, rhodopin and rhodovibrin are 99.90%, 97.77%, 98.95%, 98.74% and 97.89% before NMR experiments. UV−vis spectra of carotenoids also provide evidence of their purity. Electronic absorption spectra of carotenoids in Figure 1 show that $1^1B_u^+(1) \leftarrow 1^1A_g^-(0)$ absorptions for each carotenoid in hexane are very close to the reference value[16] and cis peaks around 375 nm are very small, indicating that the carotenoids are in all-*trans* configuration. This was confirmed by NMR ^{1}H-^{1}H ROESY NMR spectra (*vide infra*).

3.2. Construction of Initial Input Structures of Carotenoids. The chemical structures and chemical shifts both ^{1}H and ^{13}C of carotenoids are presented in Figure 2. Because these five carotenoids are synthesized in the same biosynthetic pathway, their chemical structures are very similar.

If we only consider half of the molecule of each carotenoid, their structures can be classified into three groups termed as group A, B, and C, respectively (see Figure 2). Thus, the molecules of lycopene and spirilloxanthin consist of two group A and two group B, respectively, forming symmetrical structures, while other asymmetrical carotenoids are formed by two different groups. This classification simplifies the establishment of initial input structure of carotenoids greatly.

The chemical shifts of each proton labeled in Figure 2 were assigned by the combination of ^{1}H-^{1}H COSY, ^{1}H-^{1}H long-range COSY, ^{1}H-^{1}H ROESY and was cross checked by ^{1}H-^{13}C COSY. Generally, COSY reveals the correlation of two different protons that are connected by carbon−carbon bond. ROESY, on the other hand, is caused by dipolar cross-relaxation between nuclei in a close spatial relationship. Therefore, it reveals stereochemical information of molecule, such as *exo*/*endo* and *cis*/*trans*. Figure 3 shows all the ^{1}H-^{1}H NOE relationships of carotenoids that were detected under

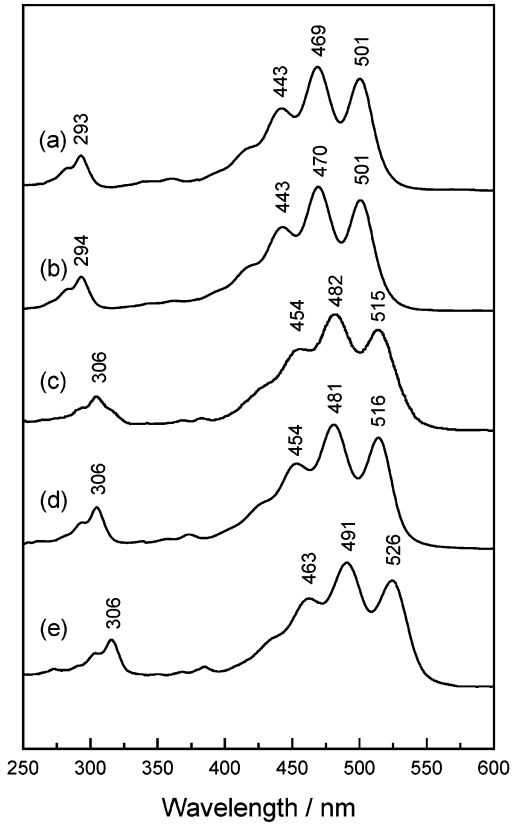

Figure 1. Electronic absorption spectra of carotenoids isolated from *Rh. marinum*: (a) lycopene; (b) rhodopin; (c) anhydrorhodovibrin; (d) rhodovibrin; and (e) spirilloxanthin. All spectra were recorded at room temperature in *n*-hexane just before NMR measurements.

the proposed experimental conditions. Based on this information, the 3-D structures of carotenoids can be described qualitatively as follows: (1) Polyene region. Because the π electrons in this region tend to delocalize, the molecule only can take *cis* or *trans* configurations. The correlation of protons in the conjugated region as well as the correlation between methyl protons and the nearest protons on the polyene chain clearly indicate that the carbon frame of polyene is in an all-*trans* configuration. The dihedral angle of four connected carbon atoms among the olefinic region can be assigned to 180° and the dihedral angle between methyl carbon and olefin carbon can be given to 0° reasonably.

(2) Terminal part of group A. This part includes C1−C5 with two methyl groups C16, C17. It has three single bonds, i.e., C2−C3, C3−C4 and C4−C5. The NOE signal between C16 and C2 protons indicates that C16 and C2 are on the same side. Due to the double bond of C1═C2 and C5═C6, the dihedral angles of C17−C1−C2−C3 and C4−C5−C6−C7 can be assigned 0° and 180°. Dihedral angle of C3−C4−C5−C6 has three possible values corresponding to 0°, −109/109° and 180°. The weak correlation signal between C3, C18 and C3, C17 protons supports the fact that C3 takes the "slightly up-direction", i.e., about −109° (same side as methyl group). This signal also can be used to assign the dihedral C3−C4−C5−C18 to 0° initially. (3) Terminal part of group B. In this group, the conjugated region extends to C3. Only three dihedral angles, O−C1−C2−C3, Me-O−C1−C2 and C1−C2−C3−C4 can be varied because of the single bond of C1−C2, O−C1 and C1−C2. A strong single

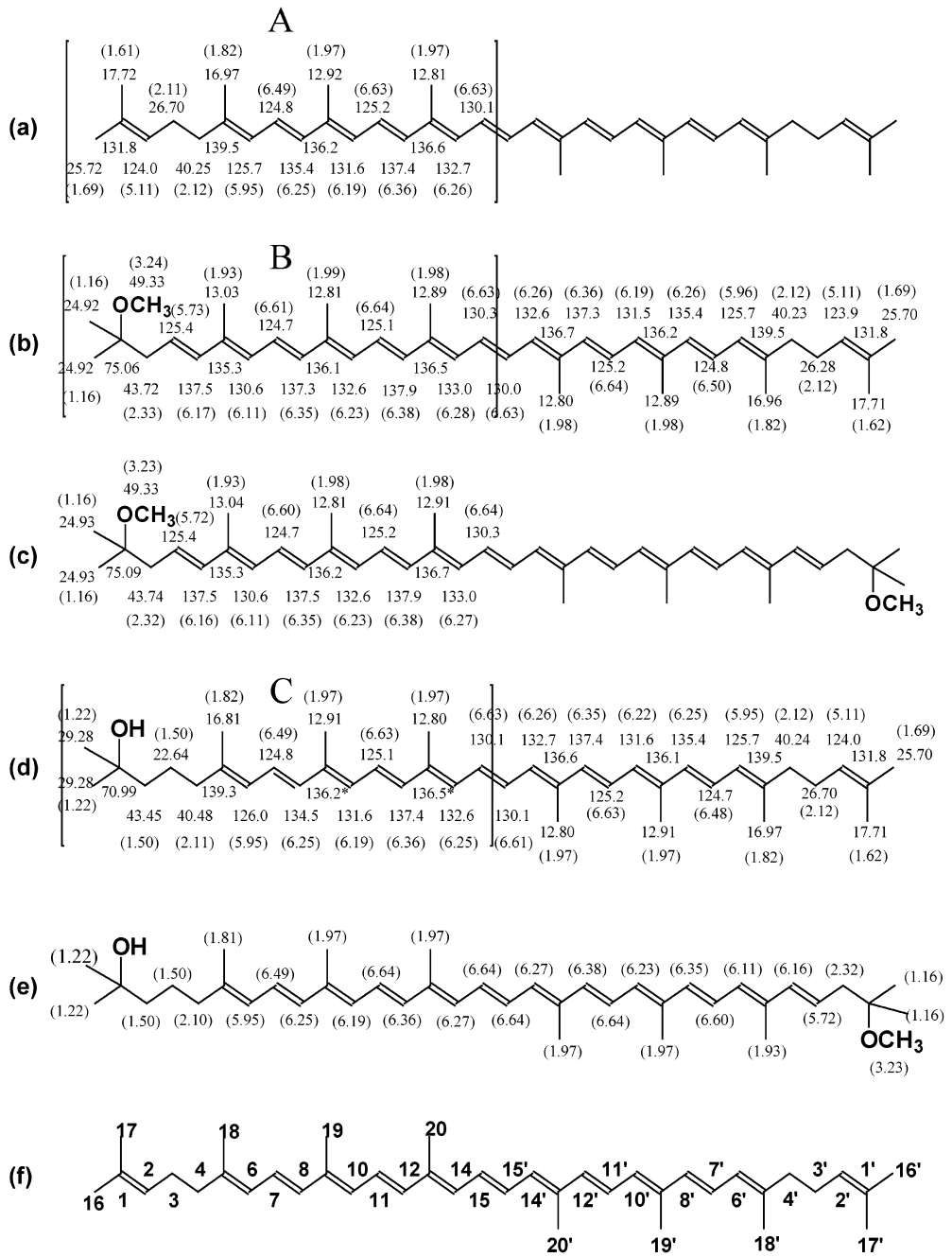

Figure 2. Chemical structure of investigated carotenoids: (a) lycopene; (b) anhydrorhodovibrin; (c) spirilloxanthin; (d) rhodopin; and (e) rhodovibrin. The ^{13}C chemical shifts are labeled in a normal way, while corresponding chemical shifts of protons are labeled in parentheses. Because of the symmetry structure of (a) and (c), only half of them are labeled. Square parentheses labeled A, B and C indicate the structure of different groups. The numbering system is shown in (f). The values labeled with an asterisk may be an alternative with their corresponding positions on another side of the molecule because the two peaks are too close to be resolved under proposed experimental conditions.

^1H signal at 1.16 ppm and ^{13}C signal at 24.93 ppm corresponding to 16, 17 methyl groups indicates that C16 and C17 methyl groups have the same chemical environments. A NOE signal between methoxy protons and 16,17 methyl protons implies that C16−C1−O-Me and C17−C1−O-Me can be assigned to 60°/−60°. The correlation between C3 and C16, C17 protons clearly shows that the dihedral angle of C3−C2−C1−O should be assigned to 180° instead of 0°. The above structural information is enough to establish the initial structure of group B. (4) Terminal part of group C. C16 and C17 protons have same chemical shifts, 1.22 ppm of ^1H and 29.28 ppm of ^{13}C, indicating that they have the same chemical environments. No correlation signal can be detected between C3 and C16, C17 protons suggesting that O−C1−C2−C3 is around 0°. No correlation of C18 and C3 protons seems that C3−C4−C5−C6 should be more than 109° (C3 takes "slightly down position", *vide supra*). But the weak signal between C2 and C4 helps to assign −109° to C3−C4−C5−C6 and 180° to C1−C2−C3−C4 roughly. (5) Whole molecule. Theoretically, the chemical shift of ^1H and ^{13}C of a molecule reflect the chemical environment of atoms in a molecule. The chemical shift of atoms can be calculated if one knows their shielding constant (σ). The chemical shifts of ^1H and ^{13}C from lycopene and

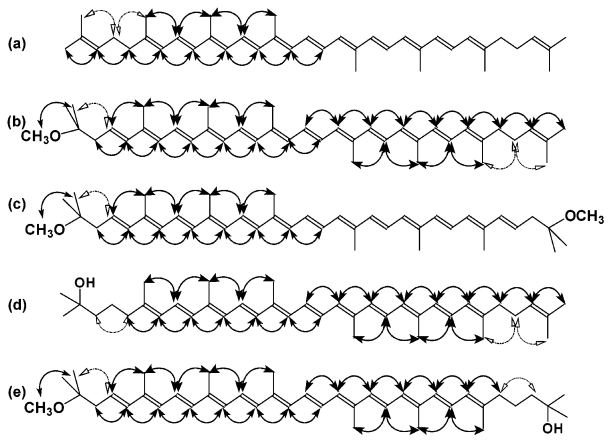

Figure 3. ^{1}H-^{1}H NOE relationships of carotenoids determined by 2-D ^{1}H-^{1}H ROESY. The protons connected by double-head arrows means they are correlated under the present experimental conditions. Empty arrows refer to weak correlations: (a) lycopene; (b) anhydrorhodovibrin; (c) spirilloxanthin; (d) rhodopin; and (e) rhodovibrin.

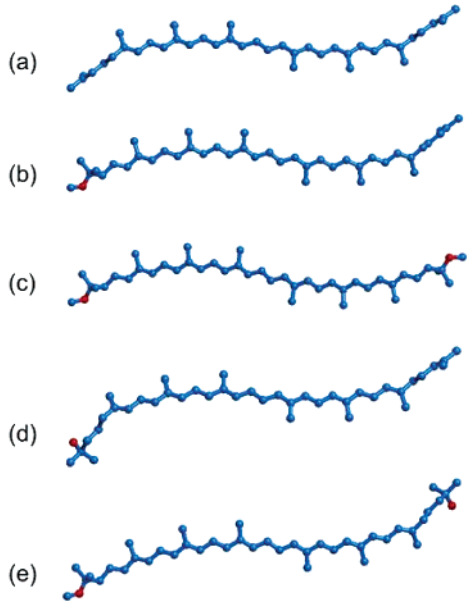

Figure 4. Optimized molecular models calculated by AM1 method based on the initial input established with NOE correlations: (a) lycopene; (b) rhodopin; (c) anhydrorhodovibrin; (d) spirilloxanthin; and (e) rhodovibrin. For the purpose of clarity, only heavy atoms are shown (blue: carbon; red: oxygen).

spirilloxanthin clearly show that the left side and right side have same values. It strong suggests that these two molecules have C_i symmetry in the solution. This C_i symmetry, therefore, was applied to lycopene and spirilloxanthin when they were constructed by the combination of two groups. Both ^{1}H and ^{13}C chemical shifts of same group in different molecules have very similar values, suggesting that same group in different molecules keeps almost the same structures or one-half of the molecule hardly affects the other half. This fact supports the idea that the other three carotenoid molecules can be constructed by using different groups only with the assumption that they have a rough C_i symmetry in the solution.

3.3. AM1 Optimized Geometries. First of all, rough structures established by NMR signals were used for initial input to obtain one of possible stable conformers. The detailed 3-D structural information, which includes bond lengths, bond angles and dihedral angles of investigated carotenoids, was then obtained by geometry optimization. Correspondent optimized molecules are shown in Figure 4. These optimized molecules support the fact that the same group in the different carotenoid molecules has very similar structure. Therefore, only three different groups' structural parameters are necessary to depict the structural characteristics of five involved carotenoids. They are listed in Table 1. By rotating one or two key dihedral angles of terminal groups, other possible stable conformers were obtained (*vide infra*).

3.3.1. Polyene Chain. The number of conjugated carbon−carbon double bonds of investigated carotenoids varies from 11 to 13. Considering the different situations of a molecule isolated in a vacuum and packed in crystal, with which AM1 calculation and X-ray determination are performed respectively, the computational results coincide with X-ray data[17,18] remarkably well in the polyene region, i.e., (1) This region is distorted in-plane distinctly forming an S-shape carbon frame due to the spatial repulsion of methyl groups (see Figure 4); (2) The distance of C═C and C−C is alternated with averaged values of 1.35 and 1.44 Å; (3) The bond attached to a methyl group is slightly longer than the nonmethylated bond both in C═C and C−C, forming four type C−C bonds. Like bond length, four different types of bond angles as well as the dihedral angle are changed periodically within the conjugated region. Here, we use types A, B, C and D to define these four different types of bond length, bond angle and dihedral angle (see Table 2). The statistic averaged bond lengths, bond angles and dihedral angles of optimized data are shown in Table 2. The relevant data of β-carotene[17] and canthaxanthin[18] obtained from their crystals are also listed in the table for comparison. For the bond lengths, calculated results show that when a methyl group was attached, the bond length becomes slightly longer. It is the same as the results in ref 13. In the case of the bond angle, the values of four different types have the order of type A < type B < type C < type D. Similar changing tendency can be seen in the X-ray data. Actually, it is these changes that result in the S-shape of carotenoids in the conjugated region. The dihedral angles are slightly away from the "optimized value" of 180°, indicating that the conjugated region is twisted out of the plane. The most pronounced deviations come from the dihedral angles, on which a methyl group is attached in the middle, i.e., type C. The calculated values varied from 172 to 177° partly because of the freely rotatable middle C−C bond. Similar things can be observed in the X-ray data. The direct cause of these periodical changes is the attachment of methyl groups in the polyene region. They change the chemical environments of carbon atoms of polyene chain. Periodical change of ^{13}C chemical shifts in this region is the solid evidence (see Figure 2). Similar statistic analysis on other conformers was performed, but no distinct differences can be found among them (data not shown).

3.3.2. Terminal Part of Group A. The terminal part of this group includes C1−C5. Because of the single bonds of C2−C3, C3−C4 and C4−C5, the terminal part of the group can rotate freely, but the dihedral angle of C3−C4−C5−C6 is a key parameter because it decides the extending direction of the terminal part. The optimized structure shows

Table 1. Optimized Structural Parameters of Groups A, B and C Based on the Initial Inputs Established with NOE Signals

				group A	group B	group C
			Bond Lengths (Å)			
C(2)	C(1)			1.343	1.539	1.514
C(3)	C(2)			1.481	1.481	1.523
C(4)	C(3)			1.519	1.341	1.518
C(5)	C(4)			1.491	1.453	1.491
C(6)	C(5)			1.348	1.357	1.348
C(7)	C(6)			1.445	1.443	1.445
C(8)	C(7)			1.346	1.347	1.346
C(9)	C(8)			1.456	1.451	1.456
C(10)	C(9)			1.354	1.358	1.354
C(11)	C(10)			1.442	1.443	1.442
C(12)	C(11)			1.348	1.347	1.348
C(13)	C(12)			1.455	1.451	1.455
C(14)	C(13)			1.354	1.358	1.354
C(15)	C(14)			1.441	1.441	1.441
C(15′)	C(15)			1.350	1.350	1.35
C(16)	C(1)			1.482	1.521	1.514
C(17)	C(1)			1.483	1.523	1.514
C(18)	C(5)			1.482	1.484	1.482
C(19)	C(9)			1.483	1.484	1.482
C(20)	C(13)			1.483	1.484	1.482
O	C(1)				1.441	1.429
O	Me				1.413	
			Bond Angles (deg)			
C(3)	C(2)	C(1)		123.4	113.389	109.5
C(4)	C(3)	C(2)		111.9	122.479	110.8
C(5)	C(4)	C(3)		111.6	126.132	111.6
C(6)	C(5)	C(4)		120.6	118.697	120.6
C(7)	C(6)	C(5)		124.6	125.382	124.7
C(8)	C(7)	C(6)		122.4	122.056	122.3
C(9)	C(8)	C(7)		124.9	125.906	125.0
C(10)	C(9)	C(8)		118.8	118.666	118.8
C(11)	C(10)	C(9)		126.5	125.558	126.6
C(12)	C(11)	C(10)		122.0	122.04	121.9
C(13)	C(12)	C(11)		124.9	125.836	125.1
C(14)	C(13)	C(12)		118.8	118.681	118.7
C(15)	C(14)	C(13)		126.5	125.607	126.6
C(15′)	C(15)	C(14)		122.3	122.472	122.2
C(16)	C(1)	C(2)		121.8	111.014	109.5
C(17)	C(1)	C(2)		122.2	111.054	109.5
C(18)	C(5)	C(4)		116.3	120.505	116.2
C(19)	C(9)	C(8)		117.0	120.29	117.0
C(20)	C(13)	C(12)		117.0	120.054	117.0
O	C(1)	C(2)			102.7	107.5
Me	O	C(1)			115.4	
			Dihedral Angles (deg)			
C(4)	C(3)	C(2)	C(1)	−171.4	137.5	173.1
C(5)	C(4)	C(3)	C(2)	179.5	177.9	175.3
C(6)	C(5)	C(4)	C(3)	−107.2	177.2	−105.2
C(7)	C(6)	C(5)	C(4)	−179.3	−179.3	−179.5
C(8)	C(7)	C(6)	C(5)	−179.0	−176.2	−175.8
C(9)	C(8)	C(7)	C(6)	180.0	−179.6	180.0
C(10)	C(9)	C(8)	C(7)	−174.2	−177.3	−172.3
C(11)	C(10)	C(9)	C(8)	179.4	179.3	179.5
C(12)	C(11)	C(10)	C(9)	179.0	175.7	−178.2
C(13)	C(12)	C(11)	C(10)	180.0	180	180.0
C(14)	C(13)	C(12)	C(11)	−177.5	−177.4	178.4
C(15)	C(14)	C(13)	C(12)	179.6	179.2	180.0
C(15′)	C(15)	C(14)	C(13)	−179.0	174.7	−177.3
C(16)	C(1)	C(2)	C(3)	180.0	−52.5	178.5
C(17)	C(1)	C(2)	C(3)	0.4	71.3	56.6
C(18)	C(5)	C(4)	C(3)	73.4	−1.1	75.3
C(19)	C(9)	C(8)	C(7)	5.7	1.1	7.4
C(20)	C(13)	C(12)	C(11)	2.5	1.0	1.6
O	C(1)	C(2)	C(3)		−171.5	−63.3
Me	O	C(1)	C(2)		171.1	

that the dihedral angle of C3−C4−C5−C18 is 73.4°, indicating methyl groups C18 and C3 are still on the same side after optimization, although it is twisted. That is why the weak NOE correlation between C18 and C3 protons can be detected. 0.4° of C17−C1−C2−C3 and −171.4° of C4−C3−C2−C1 indicate that methyl C17 and C3 is also on the same side, resulting in the correlation between C17, C3. These conformations also result in the different chemical shifts of C16 and C17 methyl groups both in ^{1}H and ^{13}C.

To find other stable conformers of the molecule, the dihedral of C3−C4−C5−C6 was rotated from 0° to 360° with a 5° interval. Each step was optimized with freedom of all parameters except that of rotated C3−C4−C5−C6. The heat of formation in each step was plotted against the dihedral angle of C3−C4−C5−C6 to form Figure 5, which clearly shows three minima labeled AA, AB and AA′. The calculation was performed on the molecule of lycopene with C_i restriction. Because of the C_i symmetry of molecule, only two minima are independent, i.e., position AA and AB corresponding to −105° and 5° of C3−C4−C5−C6. AA′ is only a symmetrical point of AA representing same conformer. Obviously, AA (or AA′) is the same as the conformer that was predicted by initial input established with NOE signals. The potential barrier from conformer AB to AA is only 0.76 kcal/mol, indicating that conformer AB is a metastable conformer which is easily changed into conformer AA even at room temperature. Most molecules, therefore, will take conformation AA.

3.3.3. Terminal Part of Group B. The conjugated region in this group extends to C3. The conformation of end part, therefore, is decided by C1−C2−C3−C4 and C3−C2−C1−OMe (or C3−C2−C1−C16/C17). The dihedral angle, −171.5°, of C3−C2−C1−OMe (or C3−C2−C1−C16/C17 of −52.5°/71.3°) clearly shows that the methoxy group is on the opposite side of the methyl group. The dihedral angles of C16−C1−O-Me/C17−C1−O-Me stayed at 71.4°/−51.7°, slightly away from the initial values of 60°/−60° to balance the methoxy group against its opposite big hydrocarbon group. This final optimized conformation is coincident with NMR observation.

The other possible potential minimum can be found by rotating both dihedral angles of C1−C2−C3−C4 and MeO−C1−C2−C3. Again, to simplify calculation, symmetrical molecule of spirilloxanthin was taken as a calculation model. Three minima labeled BA, BB, and BC can be seen in the formation energy surface of Figure 6. The other three minima BA′, BB′ and BC′ are only their symmetrical points. The Figure 6 and calculation summary listed in Table 3 reveal following facts: (1) Three local minima have the order of BA<BB<BC in terms of heat of formation. (2) Higher potential barriers between different conformers make them possible to exist in solution simultaneously. (3) Most possibly, the NOE signal between C3 protons and C16, C17 protons was produced by conformer BB, in which C3 and C16, C17 protons are on the same side although BB is not the most stable conformer.

3.3.4. Terminal Part of Group C. The conjugated length is the same as group A, but the terminal part is changed due to the hydration at C1−C2. The terminal part, therefore, becomes more flexible. The dihedral angle of C3−C4−C5−C18, which was changed from the initial value of 60° to 75.3° shows that the extending direction of the terminal part is similar with group A but more twisted (see Figure 4d). This may be one of the reasons why the NOE correlation between C18 protons and C3 protons cannot be detected.

A similar rotating calculation was performed using a molecule of rhodopin as a model. The calculated heat of

Table 2. Averaged Structural Parameters in Polyene Region of Carotenoids

	Bond distance (Å)				Bond angle(°)				Dihedral angle(°)			
	A	B	C	D	A	B	C	D	A	B	C	D
Lycopene	1.352(2)	1.443(2)	1.348(2)	1.456(1)	118.8(0)	122.2(2)	124.9(0)	126.5(1)	178.7(6)	180.0(0)	175.8(20)	179.5(2)
Anhydrorhodovibrin	1.353(2)	1.442(2)	1.348(1)	1.455(1)	118.9(0)	122.2(2)	124.9(0)	126.3(1)	177.1(8)	179.7(2)	170.7(14)	179.0(1)
Spirilloxanthin	1.358(1)	1.442(1)	1.348(2)	1.451(0)	118.7(0)	122.2(2)	125.5(2)	125.9(1)	176.4(14)	179.8(2)	177.4(10)	179.2(0)
Rhodopin	1.352(3)	1.443(1)	1.347(1)	1.456(0)	118.8(1)	122.2(2)	124.9(1)	126.5(1)	177.3(13)	180.0(0)	176.7(29)	179.7(3)
Rhodovibrin	1.353(2)	1.442(2)	1.348(2)	1.455(0)	118.9(1)	122.3(2)	124.8(1)	126.3(1)	178.5(12)	179.9(2)	170.4(35)	178.9(3)
β-carotene	1.352(3)	1.444(4)	1.350(3)	1.445(1)	118.4(9)	123.0(21)	126.7(8)	127.5(3)	176.4(21)	176.0(3)	177.5(32)	178.5(32)
Canthaxanthin	1.362(7)	1.448(6)	1.351(8)	1.456(1)	117.7(8)	123.0(16)	125.9(2)	127.2(5)	176.7(7)	177.2(6)	172.8(36)	178.7(14)

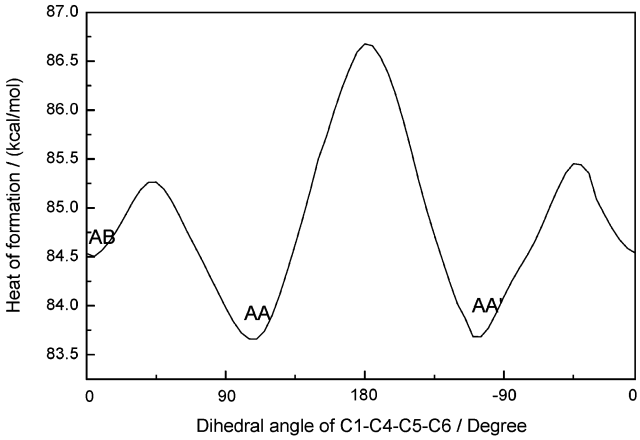

Figure 5. The curve of heat of formation calculated on the molecule of lycopene with C_i symmetry restriction.

formation curve is shown in Figure 7. An asymmetry heat formation curve is caused by asymmetrical end-groups of a molecule. Conformer CA has its two end-groups on opposite sides against the molecular plane, while conformer CB has its two end-groups on the same side. According to the heat of formation of conformers, it is reasonable to make the following two conclusions. (1) C_i symmetrical conformation is more stable than C_2 symmetrical conformation. (2) Conformer CA is the most stable one because conformer CC can easily change into CA.

Table 3. Conformation Searching Results of Group B

conformer	heat of formation (kcal/mol)	dihedral angle of O−C1−C2−C3	dihedral angle of C1−C2−C3−C4	barrier height (kcal/mol)
BA	18.9	65.0	135.0	
BB	19.8	−170.0	135.0	2.8 (BB→BA)
BC	21.4	−65.0	135.0	2.2 (BC→BB)

The AM1 geometrical optimizations show that the most stable conformer of groups A, B and C are AA, BA and CA, respectively. By using the above information, the initial inputs for the most stable conformer of carotenoids in this investigation were reconstructed. The geometry optimization was then performed again with the freedom of all degrees until the gradient norm reached 0.005. The Cartesian coordinates are supplied as Supporting Information in Tables S1−S5.

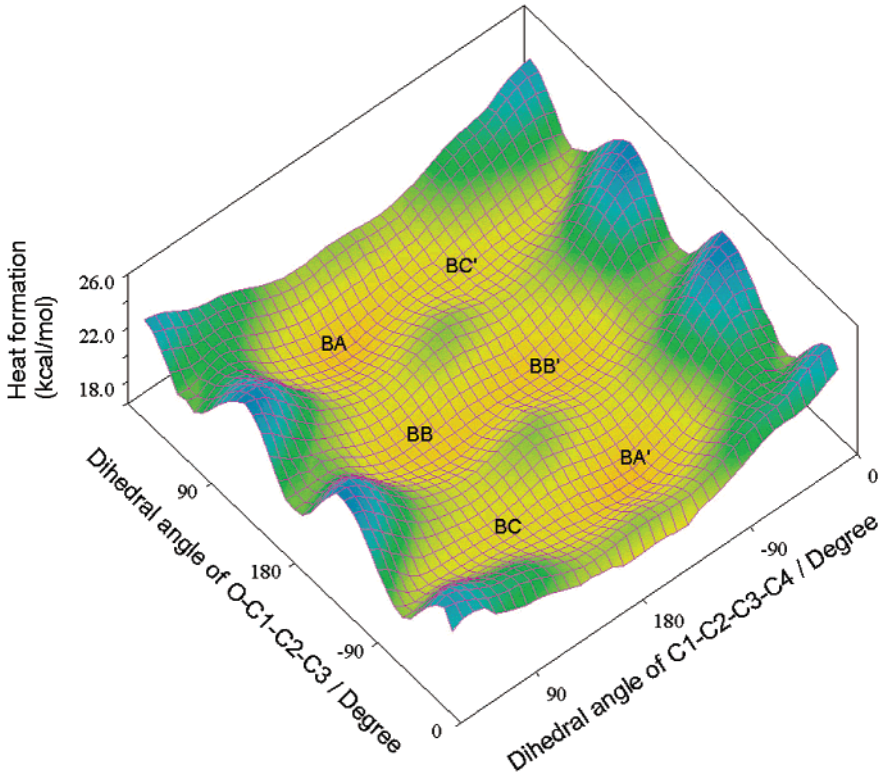

Figure 6. Potential surface of spirilloxanthin in terms of change of dihedral angles of O−C1−C2−C3 and C1−C2−C3−C4 with C_i symmetry restriction.

Table 4. Selected Dihedral Angles of Carotenoid Calculated in Free State and Bonded in Protein Crystals

	group A (deg)					group B (deg)			
	rhodopin grocoside in *Rps. acidophila*	lycopene in *Rs. molischianum* (cytoplasmic side)	lycopene in *Rs. molischianum* (periplasmic side)	lycopene in AM1 (left)	lycopene in AM1 (right)	spheroidene in *Rb. sphaeroides*	spirilloxanthin in AM1 CA	spirilloxanthin in AM1 CB	spirilloxanthin in AM1 CC
C4−C3−C2−C1	−174.0	−124.5	−163.8	173.4	−173.4	−58.0	139.7	137.5	138.3
C5−C4−C3−C2	173.6	−64.1	−173.6	−177.7	177.7	−177.7	178.2	177.9	178.2
C6−C5−C4−C3	93.6	−166.2	101.1	−109.9	109.9	−178.8	177.5	177.2	177.2
C17−C1−C2−C3	6.5	−26.1	−9.7	−0.547	0.5	−71.6	−57.2	−52.5	55.8
C16−C1−C2−C3	−160.6	138.8	−175.4	179.7	−179.7	179.3	−178.9	71.3	177.4
C18−C5−C4−C3	−98.1	4.5	−86.1	70.7	−70.7	−4.5	−1.1	−1.1	−1.1
O−C1−C2−C3						55.3	63.4	−171.5	−64.3
Me-O−C1−C2						−178.5	−171.6	171.1	−177.3

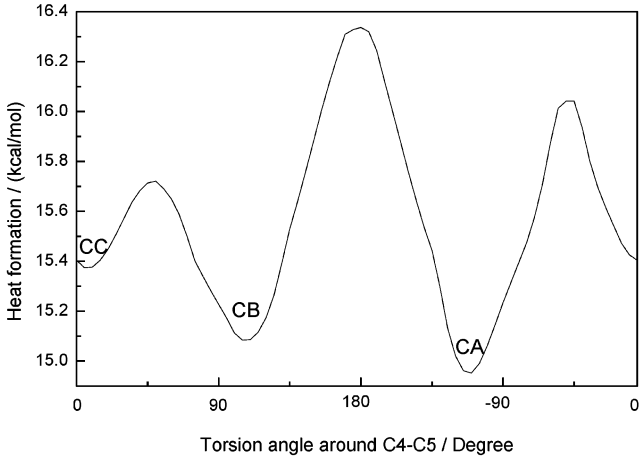

Figure 7. The curve of heat of formation calculated on the molecule of rhodopin without symmetry restriction.

3.4. Comparison of Calculated Structures of Carotenoid with that Bound in Protein Complexes. Although crystallographic data of investigated carotenoids are not available so far, some of them or half of them (groups) can be obtained from crystallographic data of photosynthetic protein complexes. It gives us a chance to make a comparison of optimized geometry with crystal structures although two main aspects have to be taken into account. (1) Carotenoid in the protein complex usually is distorted due to the interaction with the amino acid residues. (2) The resolution of X-ray data of photosynthetic protein complex crystal is only around 2−3 Å.

Light-harvesting complex II from *Rs. molischianum* contains lycopene as one of the pigments. Its crystal structure has been solved to 2.4 Å.[19] Rhodopin glucoside, which is involved in LH2 crystal of *Rps. accidophila*, has a half of lycopene (group A).[20] The crystal of the reaction center from *Rb. sphaeroides* including a 15-cis spheroidene, which has a half of spirilloxanthin (group B) is also available.[21] Table 4 compares dihedral angles of the "terminal part" of carotenoids between calculated in free state and bounded in protein crystal. It is interesting to note that conformations of group A in rhodopin glucoside and group A in lycopene (on periplasmic side) involving in LH2 crystal are very similar with the computational results. But another side of the lycopene molecule in crystal (on cytoplasmic side) behaves very different from conformations indicating that lycopene molecules in light-harvesting complexes have lost their C_i symmetry. Possibly, this is due to the interaction between carotenoid and aromatic amino acids. In the cytoplasmic side, there are 9 aromatic amino acids in close contact with the lycopene molecule, while in the periplasmic side, only one.[6] In the case of group B, the conformation of crystal of terminal part is very similar with conformer CA. The big difference between them is dihedral angle C1−C2−C3−C4. In the crystal, it is only −58.0°, indicating that there is a big distortion here. This twisted molecule may also be caused by the interaction with aromatic amino acids because two big groups in the *trans* position (139.7°) are more stable than the *cis* position (−58.0°) structurally. For the group C, the similar 3-D crystal data are still not available.

4. CONCLUSIONS

Five carotenoids in the purple photosynthetic bacterium of *Rh. marinum* were purified for conformation determination based on the ^{1}H and ^{13}C NMR measurements. The chemical structural information is used to establish the initial input for the semiempirical quantum chemical calculation program, AM1. The optimized 3-D structures subsequently obtained are in remarkably good agreement with X-ray crystallographic data. AM1 calculation and NMR results lead to the following conclusions: In the conjugated region, purified carotenoids from the purple bacteria *Rh. marinum* are in an all-trans configuration. Spatial repulsion of methyl groups causes distinct in-plane and slight out-plane distortion forming S-shape carbon backbone. Four different types of bond length, bond angle and dihedral angle changed alternately in the polyene region due to the attachment of methyl groups. For the terminal parts of carotenoids, several different conformations occur due to the rotation of single bonds. To minimize potential energy, they prefer to take extending conformations forming C_i symmetrical structure. This method, using NMR to produce initial input structure of carotenoids for theoretical calculations, provides a reliable way to determine conformations of carotenoids. It can be applied to other molecules.

ACKNOWLEDGMENT

The author thanks Prof. Y. Koyama for his encouragement and supports, Dr. H. Hashimoto for assistance with calculations. The authors are grateful to Dr. M. J. Conroy for carefully reading the manuscript as well as for useful discussions. This work has been supported by grants from The Science Research Fund and Japan Society for the Promotion of Science.

Supporting Information Available: Cartesian coordinates of the most stable structure of lycopene, anhydrorhodopin, spirilloxanthin, rhodopin, and rhodovibrin (Tables

S1−S5). This material is available free of charge via the Internet at http://pubs.acs.org.

REFERENCES AND NOTES

(1) Frank, H. A.; Cogdell, R. J. Photochemistry and function of carotenoid in photosynthesis. In *Carotenoids in Photosynthesis*; Young, A., Britton, G. Eds.; Chapman & Hall: London, 1996; pp 252−326.

(2) Imhoff, J. F. *Rhodopseudomonas marina* sp. nov., a new marine phototrophic purple bacterium. *System. Appl. Amicrobiol*. **1983**, *4*, 512−521.

(3) Meckenstock, R. U.; Brunisholz, R. A.; Zuber, H. The light-harvesting core-complex and the B820-subunit from *Rhodopseudomonas marina.* Part I. Purification and characterization. *FEBS Lett*. **1992**, *311*, 128−134.

(4) Meckenstock, R. U.; Krusche, K.; Brunisholz, R. A.; Zuber, H. The light-harvesting core-complex and the B820-subunit from *Rhodopseudomonas marina*. Part II. Electron microscopic characterisation. *FEBS Lett*. **1992**, *311*, 135−138.

(5) Qian, P.; Yagura, T.; Koyama, Y.; Cogdell, R. J. Isolation and purification of the reaction center (RC) and the core (RC-LH1) complex from *Rhodobium marinum*: the LH1 ring of the detergent-solubilized core complex contains 32 bacteriochlorophylls. *Plant Cell Physiol*. **2000**, *41*, 1347−1353.

(6) Qian, P.; Saiki, K.; Mizoguchi, T.; Hara, K.; Sashima, T.; Koyama, Y. Time-Dependent Changes in the Composition of Carotenoids Bound to the Reaction Center and the LH1 Antenna Complex from *Rhodobium marinum*: Preferential Binding of Spirilloxanthin to the Reaction Center. *Photochem. Photobiol.* **2001**, *74*, 444−452.

(7) Liaaen-Jensen, S.; Cohen-Bazire, G.; Nakayama, T. O. M.; Stanier, R. Y. The path of carotenoid synthesis in a photosyntheticbacterium. *Biochim. Biophys. Acta* **1958**, *29*, 477−498.

(8) Liaaen-Jensen, S.; Cohen-Bazire, G.; Stanier, R. Y. Biosynthesis of carotenoids in purple bacteria: A reevalution based on considerations of chemical structure. *Nature (London)* **1961**, *192*, 1168−1172.

(9) Englert, G. NMR of carotenoids: novel experimental techniques. *Pure Appl. Chem.* **1991**, *61*, 59−70.

(10) Englert, G. NMR spectroscopy. In *Carotenoids*; Britton, G., Liaaen-Jensen, S., Pfander, H., Eds; Birkhäuser Verlag: Basel, 1995; Vol. 1B, pp 225−260.

(11) Connors, R. E.; Burns, D. S.; Farhoosh, R.; Frank, H. A. Computational studies of the molecular structure and electronic spectroscopy of carotenoids. *J. Phys. Chem.* **1993**, *97*, 9351−9355.

(12) Dolan, P. M.; Miller, D. M.; Cogdell, R. J.; Brige, R. R.; Frank, H. A. Linear dichroism and the transition dipole moment orientation of the carotenoid in the LH2 antenna complex in membranes of *Rhodopseudomonas acidophila* strain 1005. *J. Phys. Chem. B* **2001**, *105*, 12134−12142.

(13) Weesie, R. J.; Merlin, J. C.; Lugtenburg, J.; Britton, G.; Jansen, F. J. H. M.; Cornard, J. P. Semiempirical and Raman spectroscopy studies of carotenoids. *Biospectroscopy* **1999**, *5*, 19−33.

(14) Law, C. J.; Cogdell, R. J. The effect of chemical oxidation on the fluorescence of the LH1 (B880) complex from the purple bacterium *Rhodobium marinum. FEBS Lett*. **1998**, *432*, 27−30.

(15) Kao, J.; Allinger, N. L. Conformational analysis. 122. Heats of formation of conjugated hydrocarbons by the force field method. *J. Am. Chem. Soc.* **1977**, *99*, 975−986.

(16) Britton, G. UV/visible spectroscopy. In *Carotenoids*; Britton, G., Liaaen-Jensen, S., Pfander, H., Eds.; Birkhäuser Verlag: Basel, 1995; Vol. 1B, pp 13−62.

(17) Senge, M. O.; Hope, H. Structure and conformation of photosynthetic pigments and related compounds 3. Crystal structure of β-carotene. *Z. Naturforsch.* **1992**, *47c*, 474−476.

(18) Bart, J. C. J.; MacGillavry, C. H. The crystal and molecular structure of canthaxanthin. *Acta Crystallogr*. **1968**, *B24*, 1587−1606.

(19) Koepke, J.; Hu, X.; Muenke, C.; Schulten, K.; Michel, H. The crystal structure of the light-harvesting complex II (B800−850) from *Rhodospirillum molischianum*. *Structure* **1996**, *4*, 581−597.

(20) McDermott, G.; Prince, S. M.; Freer, A. A.; Hawthornthwaite-Lawless, A. M.; Papiz, M. Z.; Cogdell, R. J.; Isaacs, N. W. Crystal structure of an integral membrane light-harvesting complex from photosynthetic bacteria. *Nature* **1995**, *374*, 517−521.

(21) Chirino, A. J.; Lous, E. J.; Huber, M.; Allen, J. P.; Schenck, C. C.; Paddock, M. L.; Feher, G.; Rees, D. C. Crystallographic analyses of site-directed mutants of the photosynthetic reaction center from *Rhodobacter sphaeroides*. *Biochemistry* **1994**, *33*, 4584−4593.

CI0255230